

QUARK NOVA INTERPRETATION OF THE 13 KEV EMISSION FEATURE SEEN IN THREE AXPS: 1E 1048.1–5937, XTE J1810–197 AND 4U 0142+61

N. Koning, D. Leahy, and R. Ouyed

Department of Physics and Astronomy, University of Calgary, Calgary, Canada

Received 2014 January 8; accepted 2014 March 7

RESUMEN

Tres pulsares de rayos X anómalos (AXPs) muestran, durante el estallido, líneas de emisión intensas en sus espectros. Notablemente, en los tres casos las líneas observadas ocurren en 13 keV. Esta coincidencia es un argumento en contra de la interpretación usual de su origen en términos de emisión protón-ciclotrón. En trabajos previos, Koning et al. han analizado la línea con una interpretación atómica para su origen, y han derivado restricciones sobre la energía en la línea y el ambiente del estallido. Con base en esos trabajos examinamos la interpretación atómica a la luz del modelo de la nova-quark para los AXPs. Encontramos que la emisión es congruente con la ubicación del disco, la composición y la temperatura esperadas alrededor de los AXPs según este modelo.

ABSTRACT

Three anomalous X-ray pulsars (AXPs) have significant emission lines in their burst spectra. Remarkably, the line occurs at 13 keV in all cases. This coincidence argues against the common proton-cyclotron interpretation of its origin. Previous work by Koning et al. has analysed the line using an atomic interpretation and derived constraints on the line energy and bursting environment. We build upon this work and examine the atomic interpretation in light of the quark nova model for AXPs. We find that the emission is consistent with the disk location, composition and temperature expected around AXPs in this model.

Key Words: stars: individual (XTE J1810–197, 4U 0142+61, 1E 1048.1–5937) — stars: magnetic field — stars: neutron

1. INTRODUCTION

Anomalous X-ray pulsars (AXPs) are objects (commonly believed to be neutron stars) with high X-ray luminosity (greater than can be explained through spin-down alone, hence “anomalous”), X-ray pulsations and a rapid spin-down rate. Many of these objects also experience periods of intense X-ray bursting reminiscent of soft gamma-ray repeaters (SGRs). The leading model explaining the characteristics of AXPs is the magnetar model (Thompson & Duncan 1995) in which a highly magnetized ($B \approx 10^{14} - 10^{15}$ G) neutron star powers the luminosity and causes the bursts through either fractures in the crust or reconnection events in the magnetosphere (see Woods & Thompson 2006, for a review). Others models have also been proposed to explain the properties of AXPs including the fall-back disk model (Chatterjee et al. 2000) and the quark nova model (Ouyed et al. 2007a,b).

Out of the approximately 13 known AXPs, three have shown a significant emission feature in the spectrum of at least one burst. Gavriil et al. (2002) first

reported an emission line in the spectrum of Burst 1 from the 2001 outburst of 1E 1048.1–5937 and later another from Burst 3 of the 2004 event (Gavriil et al. 2006)¹ Woods et al. (2005) observed an emission line in the spectrum of XTE J1810–197 and Gavriil et al. (2011) reported an emission line in Burst 6 of 4U 0142+61. The spectrum from each source is given in Figure 1 of Koning et al. (2013) and the fits (Gaussian line center and black body temperatures) are given in Table 1. What is remarkable is that in each case, the detected emission feature is at an energy of ≈ 13 keV. In the magnetar model the common interpretation is that these lines are proton-cyclotron in origin, implying a magnetic field of $\approx 2 \times 10^{15}$ G. The major challenge with this view is that since all three sources show the line at the same energy, they must all have the same magnetic field strength. Although this may just be an extraordinary coincidence, their magnetic fields have been measured through spin-down and in fact differ by

¹We will use Burst 3 from the 2004 event in this work as the error in this measurement is lower than that of the 2001 event.

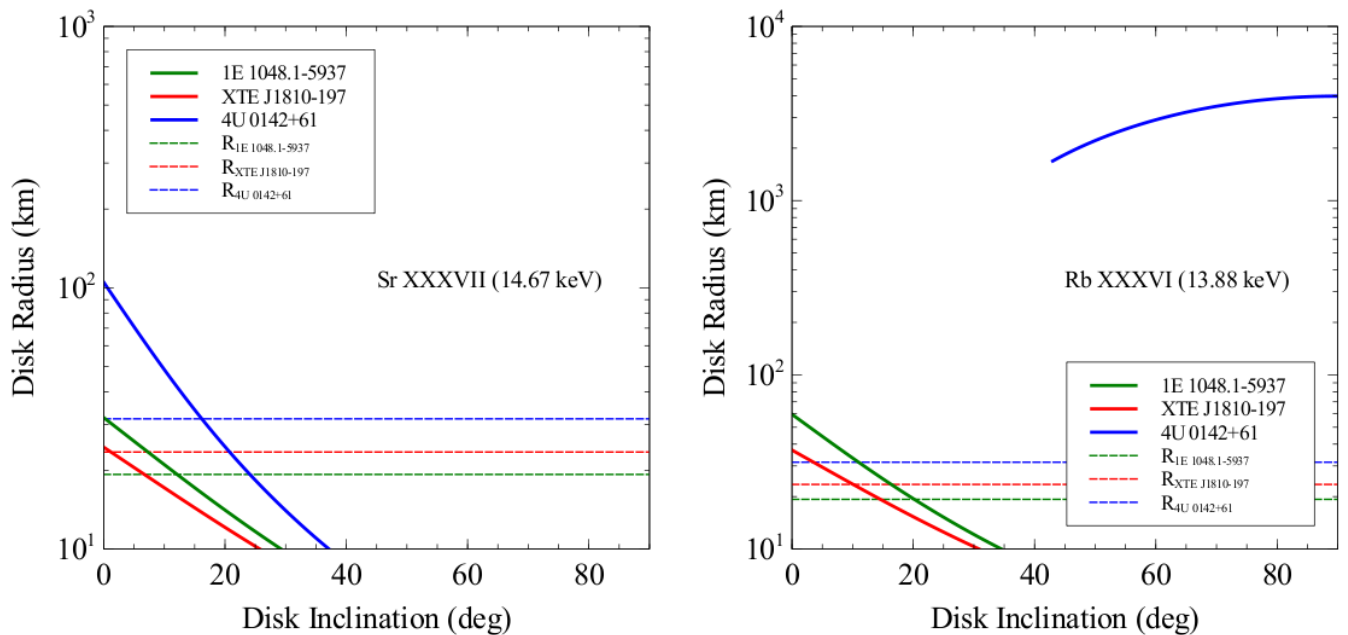


Fig. 1. Keplerian disk radius versus inclination for each AXP source using equation 4 of Koning et al. (2013). The left panel shows the possible radii and inclinations assuming the 14.67 keV transition of Sr XXXVII and the right panel assumes the 13.88 keV transition of Rb XXXVI as the source line. On each panel is shown the calculated radius of the disk, as mentioned in the text.

TABLE 1

SUMMARY OF FITS TO OBSERVED 13 KEV EMISSION FEATURES FOR EACH AXP

AXP	Line Center (keV)	T_{BB} (keV)
1E1048.1–5937 (Burst 3)	13.09 ± 0.25	2.99 ± 0.25
XTE J1810–197 (Burst 4)	12.6 ± 0.2	3.6 ± 0.2
4U 0142+61 (Burst 6)	14.2 ± 0.3	5.8 ± 0.3

a factor of 3 (Gavriil et al. 2011). This suggests that the line is probably not of cyclotron origin. Another problem with this interpretation is the odd fact that the line is seen only during some of the outbursts. For example, 4U 0142+61 went through 6 bursts and only the last showed evidence of an emission line.

An alternative approach is to consider the line as atomic. This not only gets around the coincidence problem, but presents a way in which the environment surrounding AXPs can be probed. Koning et al. (2013) performed an analysis of the 13 keV feature for each source assuming the atomic origin hypothesis. They considered three possible emission regions; a Keplerian disk in orbit around the star, a co-rotating or static region around the star and emission from the surface of the star. In each case, they were able to constrain the rest-energy of the line, giving clues as to its origin and source. In this paper we build upon and interpret these results in the context of the quark nova (QN) model for AXPs.

2. QUARK NOVA MODEL

In recent years a new theory to explain the properties of SGRs and AXPs has emerged using quark stars (QS) as the engine (Ouyed et al. 2007a,b). A QS is created through the detonation of the neutron star in a process called a quark nova (QN) (Ouyed et al. 2002; Keränen et al. 2005; Niebergal et al. 2010). The QN ejects the neutron-rich outermost layers of the neutron star (Ouyed & Leahy 2009), leading to r-process production of heavy elements (Jaikumar et al. 2007). The QN can result in heavy-element-rich material from the ejected NS crust in a Keplerian disk orbiting the remnant QS, extending from ≈ 20 km to ≈ 100 km depending on its age (Ouyed et al. 2007b). This disk is distinguished from a gaseous fall-back disk, as it is much closer to the surface of the central object, is made up of primarily degenerate material, and contains an abundance of r-process elements. A thin layer of co-rotating non-degenerate atmosphere blankets the underlying Keplerian material (see Figure 2 in Ouyed et al. 2010).

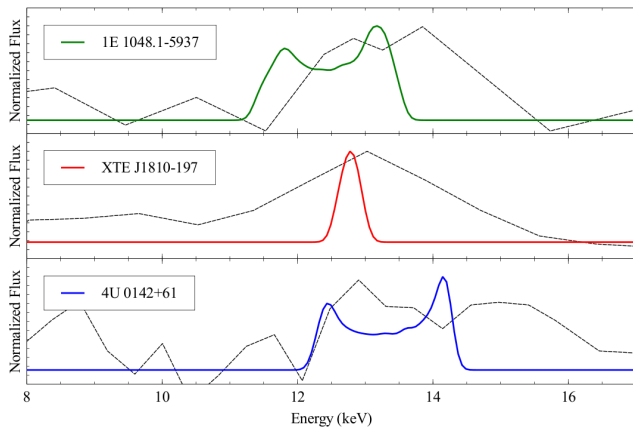


Fig. 2. Synthetic line profiles for the Keplerian disk scenario using values derived assuming Sr XXVII as the line source. Each panel displays the synthetic line profile (solid lines) for the three AXPs studies in their paper, along with the observed spectrum (dashed lines).

The quark star is born with a dipole magnetic field aligned with its axis of rotation (Ouyed et al. 2004, 2006)² and a surface magnetic field of $B \approx 10^{15}$ G (Iwazaki 2005). Many aspects of AXPs (and SGRs) have been successfully modelled using the QN scenario. The X-ray bursts are due to “chunks” of the Keplerian disk accreting onto the surface of the QS (Ouyed et al. 2007b)³ whereas the quiescent X-ray luminosity is explained by vortex expulsion (Niebergal et al. 2006) combined with steady accretion from the disk atmosphere (Ouyed et al. 2007b)⁴. In this model, the period and spin-down rate of AXPs occur through dipole spin-down and magnetic field decay following vortex expulsion (Niebergal et al. 2006). The transient radio emission seen in some AXPs can be explained by magnetic bubbles and has been successfully applied to XTE J1810–197 and 1E 1547.0–5408 (Ouyed et al. 2010). The dual component disk/QS system naturally explains the two-component spectrum seen in many AXPs.

The sequence of events during a bursting phase is outlined in Ouyed et al. (2007b) and Ouyed et al. (2010) and summarized here:

1. The shear produced by high differential velocities in the degenerate Keplerian disk causes a fracturing into discrete “walls” separated by a degenerate fluid (Ouyed et al. 2007b).
2. The magnetic field penetrates the inner wall of the Keplerian disk.

²Since the QS is an aligned rotator, we do not expect pulsed radio emission from AXPs or SGRs.

³In SGRs, a co-rotating shell is magnetically suspended above the quark star allowing for larger “chunks” to break off, leading to stronger bursting (Ouyed et al. 2007a).

⁴In the case of transient AXPs, there is no accretion during the quiescent phase (Ouyed et al. 2010).

3. The resulting magnetic torque spins down the wall so that it eventually co-rotates with the QS, separating it from the rest of the disk.
4. The inner wall accretes onto the QS releasing $\approx 10^{39} - 10^{41}$ ergs.
5. As a result, the disk is heated to temperatures $\approx 4-5$ keV.
6. Heat propagates outwards through the disk by Bohm diffusion. A new layer of non-degenerate, Keplerian material is unveiled below the co-rotating atmosphere (see Figure 2 in Ouyed et al. 2010).
7. The shear between the co-rotating disk atmosphere and the new non-degenerate Keplerian material causes ejection and accretion onto the QS, forming a hot spot.

By assuming the QN model as the engine for the three AXPs in this study, we are able to determine key features of the emitting environment.

2.1. Line Identification

The most critical aspect of this analysis is the identification of the transition responsible for the emission feature. We will assume that the same transition is responsible for the 13 keV feature in each source. Koning et al. (2013) were able to constrain the energy of the transition in both the Keplerian and co-rotating scenarios assuming a QS with $M = 1.5M_{\odot}$ and $R = 10$ km. If the emission is from a Keplerian disk, the transition must lie between ≈ 13 and ≈ 16.5 keV, and if from the co-rotating atmosphere, ≈ 14.20 and ≈ 16.88 keV.

Almost all transitions within this range of energies are from r-process elements. Although it may seem unusual for r-process elements to exist in the environment around AXPs, this is exactly what is expected in the QN model. The high neutron-to-seed ratio coupled with the high entropy of the QN explosion leads to an ideal site in the ejected neutron star crust for the r-process (Jaikumar et al. 2007). Since the disk is made up from the fall-back ejecta, it is expected to contain an abundance of r-process elements.

The strength of a line depends on many factors including the temperature and density of the emitting region and the transition probability (Einstein A coefficient). In each source, the temperature of the black body (BB) fit to the spectrum was $\gtrsim 3$ keV (see Koning et al. 2013). For an emission line to be observed on top of the BB spectrum, the emission region would have to be at a higher temperature. We can therefore assume a temperature ≥ 3 keV.

There are many elements with transitions between ≈ 13 and ≈ 16.88 keV, but very few have determined

TABLE 2

TRANSITIONS BETWEEN 13 AND 16.88 KEV FROM THE NIST DATABASE WITH NON-ZERO TRANSITION PROBABILITIES

Species	Energy (keV)	A_{ki} (s^{-1})	$E_i - E_k$ (ev)
Rb XXXVII	16.856	3.10e+14	0.00 - (16856.3376)
Sr XXXVIII	15.090	1.2834e+15	0.00 - (15089.924)
Sr XXXVIII	14.992	4.068e+10	0.00 - (14992.611)
Sr XXXVIII	14.990	1.3190e+15	0.00 - (14990.532)
Sr XXXVII	14.669	1.834e+15	0.00 - (14669.368)
Sr XXXVII	14.644	1.453e+11	0.00 - (14644.568)
Sr XXXVII	14.562	5.313e+14	0.00 - (14562.147)
Sr XXXVII	14.512	1.015e+10	0.00 - (14512.031)
Rb XXXVII	14.287	1.15e+15	0.00 - (14287.1819)
Rb XXXVII	14.198	1.18e+15	0.00 - (14198.0868)
Rb XXXVI	13.880	1.66e+15	0.00 - (13880.216)
Rb XXXVI	13.783	4.58e+14	0.00 - (13782.851)

TABLE 3

INCLINATION OF KEPLERIAN DISK FOR EACH AXP SOURCE*

AXP	$Inc_{14.67}$ (deg)	$Inc_{13.88}$ (deg)
1E1048.1–5937	12.6	20.2
XTE J1810–197	1.2	10.1
4U 0142+61	16.2	N/A

*Inclinations derived using both the Sr XXXVII line at 14.67 keV and the Rb XXXVI line at 13.88 keV are given.

TABLE 4

MASS OF THE QS*

AXP	$M_{14.67}$ (M_{\odot})	$M_{13.88}$ (M_{\odot})
1E1048.1–5937	1.33	0.72
XTE J1810–197	2.08	1.4
4U 0142+61	0.67	N/A

*Assuming emission from the co-rotating atmosphere of the disk for each axp source. Masses derived using both the Sr XXXVII line at 14.67 keV and the Rb XXXVI line at 13.88 keV are given.

transition probabilities. We will proceed by only considering transitions for which we have transition probabilities, understanding that until more atomic data are available our identifications cannot be final. The possible transitions in this range with calculated probabilities can be obtained from the NIST atomic line database and are reproduced in Table 2. From this list we see that the Sr XXXVII line at ≈ 14.67 keV is the strongest, with the transition of Rb XXXVI at ≈ 13.88 keV a close second. The ionization energy of Rb XXXV (producing Rb XXXVI) is ≈ 4.3 keV (Sansonetti 2006) and that of Sr XXXVI (producing Sr XXXVII) is ≈ 4.6 keV (Sansonetti 2011). Both of these values are consistent with the BB fits to the AXP sources. Furthermore, after the inner wall is initially accreted onto the QS, the disk is heated to ≈ 4 – 5 keV (Ouyed et al. 2010), enough for the ionization of these species.

Although it is likely that each line listed in Table 2 contributes to the observed feature in our AXPs, the peak is likely to be dominated by the strongest line. We will therefore examine the model parameters for each of the strongest lines; Rb XXXVI at 13.88 keV and Sr XXXVII at 14.67 keV.

2.2. Disk Radius

Equation 13 in Ouyed et al. (2007b) provides a means to calculate the disk radius given the quiescent luminosity (L) of the AXP source. For 4U 0142+61 ($L \approx 1.1 \times 10^{35}$ erg s^{-1}) we obtain a radius of 31.5 km, and for 1E1048.1–5937 ($L \approx 0.06 \times 10^{35}$ erg s^{-1}) we obtain a radius of 19.3 km. XTE J1810–197 is a transient source, so equation 13 in Ouyed et al. (2007b) does not apply. Ouyed et al. (2010) however calculate the radius of the disk to be ≈ 23.5 km using other means. We will assume these radii in our analysis below.

2.3. Emission Scenarios

Koning et al. (2013) provide three possible scenarios for the emitting region around the compact object (QS in our case): A Keplerian disk, a co-rotating region, and the surface of the QS. The last scenario does not apply in this model, as no species is expected to survive on the surface of a QS. The Keplerian disk of the QN model is primarily degenerate, with a thin non-degenerate atmosphere. During quiescence the atmosphere is co-rotating with the QS, whereas during a

burst it consists of both a co-rotating and a Keplerian layer. It is therefore possible that the emission region is Keplerian, co-rotating or both, making Scenarios I and II in Koning et al. (2013) equally likely.

2.3.1. Scenario I, Keplerian Atmosphere

There are two unknowns in this scenario that will effect the observed location of the line; the mass of the QS and the inclination of the disk. We will assume a mass of $1.5 M_{\odot}$ and derive the inclination.

As mentioned above, a layer of non-degenerate Keplerian material is unveiled during an AXP burst. This material is heated to 4–5 keV and is a possible site for the emission of the 13 keV feature. We can use equation 4 from Koning et al. (2013) to determine the allowed radii and inclinations of the disk for each AXP source. Figure 1 shows a plot of radius versus inclination for each source, with the left panel assuming the Sr XXXVII line and the right the Rb XXXVI line. The radii of each disk calculated above are shown as horizontal lines on the plots.

The inclination of the disk in each system is displayed in Table 3. Interestingly, for the Rb XXXVI transition, there is no inclination which corresponds to the calculated radius of 4U 0142+61. This means that there is no way to rotate the disk, given a radius of 31.5 km, which would reproduce the emission feature seen in the observations of 4U 0142+61. For this reason we conclude that the peak of the emission feature seen in these AXPs cannot be caused by the Rb XXXVI transition at 13.88 keV if the emission is from the Keplerian layer of the atmosphere. This makes the Sr XXXVII line at ≈ 14.6 keV the most likely candidate.

2.3.2. Scenario II, Co-rotating Atmosphere

Again our two unknown parameters are the inclination of the disk and the mass of the QS. In this scenario, the Doppler effect plays no significant role in the observed position of the line and therefore the inclination of the disk has no observable effect. We will therefore derive the mass of the QS.

The disk in the QN model has a thin non-degenerate, co-rotating atmosphere during both the quiescent and the bursting phase. During the burst, this atmosphere is heated to ≈ 4 –5 keV; hot enough to excite our assumed transitions of Rb XXXVI and Sr XXXVII.

In the co-rotating scenario, the line position is determined by the gravitational red-shift (Koning et al. 2013):

$$E_e = \frac{E_o}{\sqrt{1 - 2GM/c^2r}}, \quad (1)$$

where E_e is the energy of the transition, E_o is the observed energy, r is the radius of the emission region (see §2.2) and M is the mass of the QS. Knowing r and E_o , we can use Equation 1 to calculate the mass of the QS for $E_e = 13.88$ eV (Rb XXXVI) and $E_e = 14.67$ eV (Sr XXXVII). The results are presented in Table 4. Analogous to the Keplerian scenario, there is no acceptable mass for 4U 0142+61 for the Rb XXXVI case. This is obvious since the observed line, at 14.2 keV, is at a higher energy than the Rb XXXVI transition. Without a significant Doppler effect (as is the case in this scenario) there is no way to shift the line blue-ward. For this reason we conclude that Rb XXXVI cannot be the dominant transition in the co-rotating atmosphere scenario. The mass of the QS in the Sr XXXVII case (0.67, 2.08 and $1.33 M_{\odot}$ for 4U, XTE and 1E respectively) is well within theoretical limits for each AXP (see, e.g. Steiner et al. 2013).

3. DISCUSSION AND CONCLUSION

We have shown that the ≈ 13 keV emission feature observed in three AXP sources is consistent with emission from either the co-rotating or the Keplerian layer of the disk atmosphere in the QN model. The most likely transition is that of Sr XXXVII at 14.67 keV based on its ionization energy and transition strength. We have ruled out the strong Rb XXXVI transition at 13.88 keV as the main contributor to the observed feature in both scenarios. Using the Sr XXXVII line, we were able to determine the disk inclination in each system under Scenario I and the mass of the QS under Scenario II. The inclination of each disk under Scenario I is shallow; 12.6° , 1.2° and 16.2° for 1E 1048.1–5937, XTE J1810–197 and 4U 0142+61 respectively. The mass of the QS derived for Scenario II, 1.33, 2.08 and $0.67 M_{\odot}$ for 1E 1048.1–5937, XTE J1810–197 and 4U 0142+61 respectively, are all within the theoretical limits. A summary of our results is given in Table 5.

Determining where the emission comes from, either the Keplerian or co-rotating atmosphere, will require higher resolution spectra where the line shape can be better studied. Using the software SHAPE (Steffen et al. 2011), we have created synthetic spectra of each source under the Keplerian scenario using the results derived in this paper. The synthetic spectra (solid lines) are displayed in Figure 2 along with the observed spectra (dashed lines). If future observations reveal a split line similar to those shown in Figure 2, this will be an indisputable proof of a Keplerian emission region within ≈ 100 km of the compact object. If no split line is detected, the emission region can be either the co-rotating or the Keplerian atmosphere, the latter being from a disk with low inclination (e.g. XTE J1810–197, see Figure 2).

The QN model can address the problem of the detection of the line in some bursts, but not in others. As we noted above, during a burst the disk can be heated

TABLE 5
SUMMARY OF AXP PROPERTIES*

Source	Radius (km)	Keplerian Inc (deg)	Co-rotating $M_{\text{QS}} (M_{\odot})$
1E1048.1–5937	19.3	12.6	1.33
XTE J1810–197	23.5	1.2	2.08
4U 0142+61	31.5	16.2	0.67

*As determined in this paper assuming the Sr XXXVII transition at 14.67 keV.

anywhere from ≈ 4 to 5 keV depending on the mass of the wall accreted. The ionization energy of Sr XXXVI (producing Sr XXXVII) is ≈ 4.6 keV, right in the middle of the temperatures expected during a burst. It is simply possible that some bursts are energetic enough to ionize Sr XXXVI, whereas others are not.

In recent years, several known magnetars have shown evidence of low-magnetic fields using X-ray satellites (e.g. Rea et al. 2010). These “low-B” magnetars provide a good test as to whether the 13 keV line is proton-cyclotron or atomic in origin. For example, if the 13 keV emission line is detected during a burst of a low-B magnetar in the future, we can be certain it is not proton-cyclotron and the atomic interpretation will become more likely.

This work is funded by the Natural Sciences and Engineering Research Council of Canada. N.K. would like to acknowledge support from the Killam Trusts.

REFERENCES

- Chatterjee, P., Hernquist, L., & Narayan, R. 2000, *ApJ*, 534, 373
- Gavriil, F. P., Dib, R., & Kaspi, V. M. 2011, *ApJ*, 736, 138
- Gavriil, F. P., Kaspi, V. M., & Woods, P. M. 2002, *Nature*, 419, 142
- Gavriil, F. P., Kaspi, V. M., & Woods, P. M. 2006, *ApJ*, 641, 418
- Iwazaki, A. 2005, *Phys. Rev. D*, 72, 114003
- Jaikumar, P., Meyer, B. S., Otsuki, K., & Ouyed, R. 2007, *A&A*, 471, 227
- Keränen, P., Ouyed, R., & Jaikumar, P. 2005, *ApJ*, 618, 485
- Koning, N., Leahy, D., & Ouyed, R. 2013, *RevMexAA*, 49, 351
- Niebergal, B., Ouyed, R., & Jaikumar, P. 2010, *Phys. Rev. C*, 82, 062801
- Niebergal, B., Ouyed, R., & Leahy, D. 2006, *ApJL*, 646, L17
- Ouyed, R., Dey, J., & Dey, M. 2002, *A&A*, 390, L39
- Ouyed, R., Elgarøy, Ø., Dahle, H., & Keränen, P. 2004, *A&A*, 420, 1025
- Ouyed, R., & Leahy, D. 2009, *ApJ*, 696, 562
- Ouyed, R., Leahy, D., & Niebergal, B. 2007a, *A&A*, 473, 357
- _____. 2007b, *A&A*, 475, 63
- Ouyed, R., Leahy, D., & Niebergal, B. 2010, *A&A*, 516, 13
- Ouyed, R., Niebergal, B., Dobler, W., & Leahy, D. 2006, *ApJ*, 653, 558
- Rea, N., et al. 2010, *Science*, 330, 944
- Sansonetti, J.E. 2006, *J. Phys. Chem. Ref. Data*, 35
- _____. 2011, *J. Phys. Chem. Ref. Data*, 41
- Steffen, W., Koning, N., Wenger, S., Morisset, C., & Magnor, M. 2011, *IEEE Transactions on Visualization and Computer Graphics*, 17, 454
- Steiner, A. W., Lattimer, J. M., & Brown, E. F. 2013, *ApJL*, 765, L5
- Thompson, C., & Duncan, R. C. 1995, *MNRAS*, 275, 255
- Woods, P. M., & Thompson, C. 2006, *Compact stellar X-ray sources*, ed. W. Lewin, M. van der Klis (Cambridge University Press, Cambridge: ARI) 39, 547
- Woods, P. M., et al. 2005, *ApJ*, 629, 985